COPPER DOPED TITANIUM DIOXIDE (TiO_2) NANOPARTICLES FOR ENHANCED PHOTOCATALYTIC ACTIVITY UNDER VISIBLE LIGHT IRRADIATION

LEONG SHENG YAU

BACHELOR OF CHEMICAL ENGINEERING
UNIVERSITI MALAYSIA PAHANG

Thesis Access Form

No_____Location_____

Author : ……

Title : ……

Status of access OPEN / RESTRICTED / CONFIDENTIAL

Moratorium period:_____ years, ending_____/_____200____

Conditions of access proved by (CAPITALS): DR JOLIUS GIMBUN

Supervisor (Signature)……

Faculty: ……

Author's Declaration: *I agree the following conditions:*

OPEN access work shall be made available (in the University and externally) and reproduced as necessary at the discretion of the University Librarian or Head of Department. It may also be copied by the British Library in microfilm or other form for supply to requesting libraries or individuals, subject to an indication of intended use for non-publishing purposes in the following form, placed on the copy and on any covering document or label.

*The statement itself shall apply to **ALL** copies:*

This copy has been supplied on the understanding that it is copyright material and that no quotation from the thesis may be published without proper acknowledgement.

Restricted/confidential work: All access and any photocopying shall be strictly subject to written permission from the University Head of Department and any external sponsor, if any.

Author's signature…….Date: ……

users declaration: for signature during any Moratorium period (Not Open work): ***I undertake to uphold the above conditions:***			
Date	Name (CAPITALS)	Signature	Address

COPPER DOPED TITANIUM DIOXIDE (TiO_2) NANOPARTICLES FOR ENHANCED PHOTOCATALYTIC ACTIVITY UNDER VISIBLE LIGHT IRRADIATION

LEONG SHENG YAU

Thesis submitted in partial fulfilment of the requirements
for the award of the degree of
Bachelor of Chemical Engineering

Faculty of Chemical & Natural Resources Engineering
UNIVERSITI MALAYSIA PAHANG

APRIL 2013

SUPERVISOR'S DECLARATION

We hereby declare that we have checked this thesis and in our opinion, this thesis is adequate in terms of scope and quality for the award of the degree of Bachelor of Chemical Engineering.

Signature	:
Name of main supervisor	: ASSOC. PROF. DR. MAKSUDUR RAHMAN KHAN
Position	: SENIOR LECTURER
Date	: 9 JULY 2013

STUDENT'S DECLARATION

I hereby declare that the work in this thesis is my own except for quotations and summaries which have been duly acknowledged. The thesis has not been accepted for any degree and is not concurrently submitted for award of other degree.

Signature :
Name : LEONG SHENG YAU
ID Number : KA09158
Date : JANUARY 2013

Dedication

To my loving family members

ACKNOWLEDGEMENT

I would like to express my humble gratitude to the following people:

- My supervisor Assoc. Prof. Dr. Maksudur Rahman Khan for his guidance throughout my whole research.
- Puan Hamidah binti Abdullah for her guidance in sol-gel method and her help in catalyst characterization.
- Master student Nor Amalina binti Hussain who helped me with the equipment setup and her guidance on using the unit apparatuses.
- PhD student Ong Huei Ruey who taught me the synthesis of copper (Cu) salt.
- PhD student Baranitharan. E. who accompanied me during the whole experiment.
- Fellow friend, Tan Wooi Chuan who guided me on how to operate the batch reactor.
- My beloved family and friends who gave their utmost support during my whole research.

ABSTRACT

Titanium dioxide (TiO_2) is best known for its inexpensiveness and highly available as a photocatalyst. However, due to its wide-bandgap of 3.2 eV and the fast recombination of electron-hole pair, they have contributed to the inability to use the sunlight sufficiently as well as hindering for any reaction to happen. The objectives of the title are to synthesize a copper (Cu) doped TiO_2, to inspect the photocatalytic activity of the synthesized TiO_2 and to study the kinetic of the degradation of methylene blue (MB). A Cu salt is first synthesized using copper nitrate ($Cu(NO_3)$) mixed in the glycerol phase. The preparation of TiO_2 was carried out by the sol-gel method and the resulted Cu salt is added into it to in a 10 wt.% Cu/TiO_2 manner. The resulted gel was aged for a day before it was heated up in the oven for 24 hours, which resulted in powder form. It was grinded and calcinated at 300 ^oC for an hour. The photocatalytic activity of the synthesized catalyst was inspected with the degradation of methylene blue (MB). As a result, the photocatalytic activity had been increased and the $K0\,(\left(\frac{k0H}{K0}\right) + k0$ is 0.03236 mg L^{-1} min^{-1} while K_0 is 9.32615 X 10^{-3} ^4L mg^{-1}.

ABSTRAK

Titanium dioksida (TiO_2) dikenali dengan harga yang murah dan sedia ada sebagai katalis. Namun demikian, disebabkan oleh bandgapnya yang luas sebanyak 3.2 eV dan kadar elektron-lubang kombinasi kembali yang cepat, TiO_2 tidak dapat menggunakan cahaya matahari dengan effektif. Objektif kajian ini ialah untuk memasukkan kuprum (Cu) dalam TiO_2, memerhatikan photoaktiviti katalis, dan membuat kajian tentang kinetik degradasi methylene blue (MB). Pertama sekali, garam kuprum dibuat dalam gliserol fasa dan dicampurkan dengan kuprum nitrat ($Cu(NO_3)$). Katalis TiO_2 dibuatkan dengan cara sol-gel dan 10% berat Cu dimasukkan. Gel yang telah disintisis akan dibiar dalam satu hari selepas dipanaskan dalam oven selama 24 jam. Ketulan gel akan ditumbukkan and lalu dipanaskan dalam furnace selama satu jam pada tahap suhu 300 ^{o}C. Photoaktiviti katalis

diujikan dengan degradasi MB. Photoaktiviti katalis telah ditingkatkan akibatnya dan $K0$ $(\left(\frac{k0H}{K0}\right) + k0$ yang didapati ialan 0.03236 mg L^{-1} min^{-1} dan K_0 ialah 9.32615 X 10^{-3} ^{4}L mg^{-1}.

TABLE OF CONTENTS

LIST OF FIGURES

LIST OF TABLES

LIST OF ABBREVIATIONS

FTIR	Fourier Transform Infra-Red
UV-Vis	Ultraviolet/Visible
MB	Methylene Blue
C	Concentration
C_0	Initial Concentration
C_{01}	Initial Concentration of 70 ppm MB
C_{02}	Initial Concentration of 50 ppm MB
C_{03}	Initial Concentration of 30 ppm MB
C/C_0	Ratio of Current Concentration to the Respect of the Initial Concentration
C/C_{01}	Ratio of Current Concentration to the Respect of the Initial Concentration of 70 ppm MB
C/C_{02}	Ratio of Current Concentration to the Respect of the Initial Concentration of 50 ppm MB
C/C_{03}	Ratio of Current Concentration to the Respect of the Initial Concentration of 30 ppm MB
T	Temperature

1 INTRODUCTION

1.1 Motivation and statement of problem

Photocatalyst is a light-activated catalyst. When a photocatalyst is exposed to light, it absorbs photon energy and causes various chemical reactions. Metal complexes and semiconductor catalyst are recognised as photocatalyst materials (Kameyama et al, 2010). Titanium dioxide is possibly one of the best photocatalyst. This is because of its high efficiency, inexpensiveness, easy production, photochemical and biological stability, and inert to the environment and human beings (Paola et al, 2008; Bendavid et al, 1999; Ku et al, 1996). Due to these several reasons, a lot of researches were done in the development of photocatalyst as a result, it had being applied in many different fields, such as degradation of organic pollutants in water and wastewater (Wen et al, 2006; Liu et al, 2010; Yousef et al, 2011, Guo et al, 2012), as a disinfectants (Shieh et al, 2006; Chang et al, 2011), and for air-cleaning purpose (Sano et al, 2012; Dong et al, 2013).

Despite the advantages of using titanium dioxide as a photocatalyst, a major problem faced in using TiO_2 photocatalyst is its wide-bandgap of having a value of 3.2 eV (Jiang et al, 2010; Liu et al, 2011; Dong et al, 2013). The sunlight consists of only a small fraction, approximately 3-5% (Kim et al, 2012; Zou et al, 2001; Maeda et al, 2006) of ultraviolet (UV)- light, 45% of visible light (Dong et al, 2012) while the rest is infrared light. In other words, its wide-bandgap has contributed to the inability to use the sunlight sufficiently, as the 3.2 eV bandgap of TiO_2 can only be activated under the near and UV-light only. Quite simply, the rest of the light which has lower energy (wider wavelength) than UV-light is not suitable for the semiconductor electronic band gap cannot generate electron-hole pairs and

is therefore wasted as heat (Jiang et al, 2010). Another problem faced when using titanium dioxide is the fast recombination of electron-hole pair (Mills, 1997), thus hindering for any reaction to take place.

1.2 Objectives

The following are the objectives of this research:

- To synthesize the copper doped titanium dioxide.
- To inspect the photocatalytic activity of the copper doped titanium dioxide.
- To study the kinetic of the photocatalytic reaction.

1.3 Scope of this research

The following are the scope of this research:

i) Synthesizing of copper doped TiO_2 through sol-gel method.

ii) Characterization to be done with Fourier-Transform infrared spectra (FTIR).

iii) Photocatalytic test with the degradation of methylene blue (MB).

iv) Kinetic studies of the degradation of methylene blue (MB).

1.4 Main contribution of this work

The following are the contributions

- The degree of increased in the photocatalytic activity through the research will not only bring a better understanding in photocatalyst, but it will serve as a reference to the other researchers to come up with a better idea to further develop better photocatalyst in the future. This will ultimately reduce the bandgap of the titanium dioxide as well as the rate of recombination of electron-hole pair.
- This would lead the world of using photocatalyst which only utilise the sunlight for any specific reaction to happen, without the

consideration like the conventional catalyst which requires certain reaction temperature and pressure.

1.5 Organisation of this thesis

The structure of the reminder of the thesis is outlined as follow:

Chapter 2 provides a description of the fundamental of mechanism of the photocatalyst, followed by the doping of metals, how doping would helped in increasing the photocatalytic activity, and the kinetic studies.

Chapter 3 gives an insight of how the synthesized Cu salt is made before being doped into TiO_2 to create the novel synthesized Cu doped TiO_2, along with the materials and the equipments used during the research and for the kinetic studies.

Chapter 4 is gives a review of the comparison of TiO_2 and the synthesized Cu doped TiO_2. The photocatalytic test data is analysed with the aid of the graph plots. The kinetic studies is discussed here as well.

Chapter 6 draws together a summary of the thesis and outlines the future work which might be derived from the model developed in this work.

2 LITERATURE REVIEW

2.1 Overview

The activation of the semiconductor to take part in a reactor is first being explained through the excitation of the electrons from the electron valence through the bandgap and to the conduction band after absorbing a sufficient or more amount of energy from the sunlight. The two main obstructions faced in the photocatalytic reaction are the wide bandgap and the fast recombination of the electron-hole pair. Doping has so far been reported to be one of the way to curb such happenings by narrowing the bandgap to allow lower energy to be absorbed by the semiconductor for the excitation of electrons to happen. A kinetic studies of the photocatalytic activity is later discussed as well.

2.2 Introduction

For this chapter, it covers about the fundamental mechanism of the photocatalyst in semiconductor, specifically to titanium dioxide (TiO_2), later followed by the doping and how doping will affect the bandgap of TiO_2, which leads to the increase of photocatalytic activity. Kinetic study of the degradation of the methylene blue (MB) is discussed at the later part of the chapter.

2.3 Fundamental Mechanism of Photocatalyst

The fundamental mechanism of photocatalyst is the ability of a semiconductor to absorb photons creating reactive electron-hole pairs which

are capable of oxidizing most organic and inorganic compounds (Bloh et al, 2012). Often, a semiconductor is chosen for such particular reason due to its nature of having band gap, which separates both the valence band and the conduction band. Given enough energy in the form of photon provided by the light, absorbed by the semiconductor, for this case, TiO_2, the electrons in the valence band should achieve excitation state to excite from the valence band to the conduction band of the semiconductor. The energy of the photon can be calculated with the following formula:

$$E = hf$$

where E is the energy of the particle of light, called photon, h is the Planck constant of having a value of 6.63×10^{-34} Js, and f is the frequency of its associated electromagnetic wave. Simultaneously, a positively charged hole is created in the valence band. Varying reactions will take place with the surfaced adsorbed molecules (Mills et al, 1997), with the aid of these excited electrons that appear on the surface of the semiconductor in the conduction band.

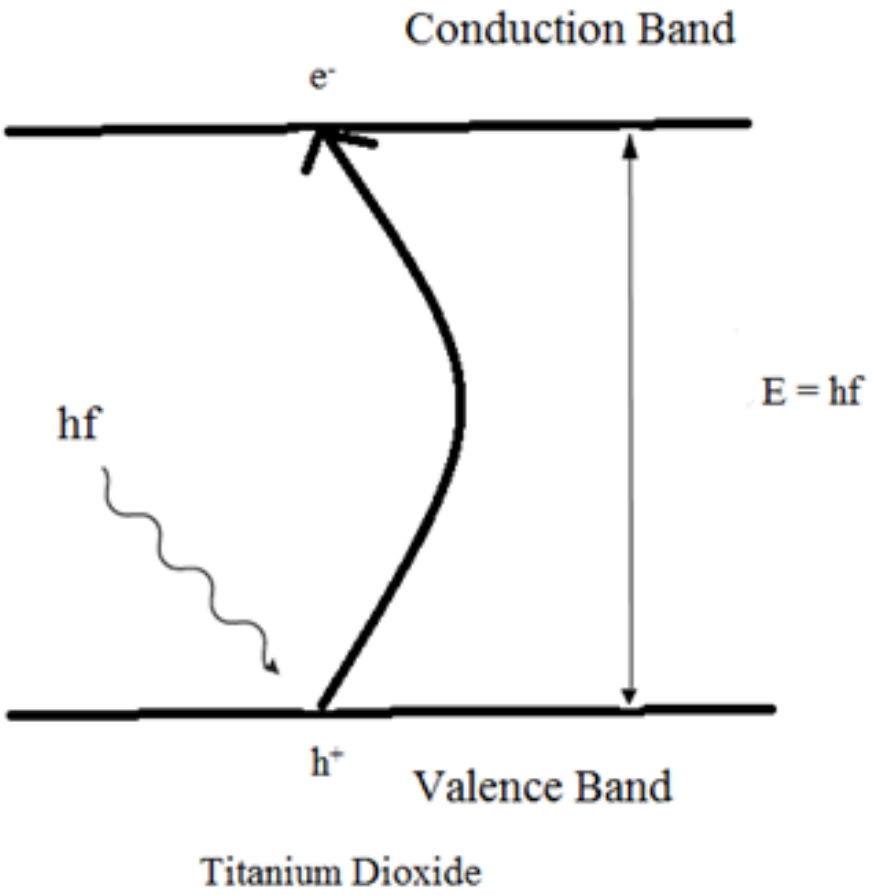

Figure 2.1: Fundamental mechanism of photocatalyst- Excitation of electron from the valence band to the conduction band.

The excited electrons in the conduction band which are responsible to carry out a reaction. Another point which is worth noticing is that due to the nature of bandgap, the photo-generated electrons in the bottom of the conduction band can have the sufficient negative redox potential to drive any reaction of lesser negative redox potential (Jiang et al, 2012). The reduction of carbon dioxide (CO_2) is one of the application that uses this feature of TiO_2 to carry out the experiment. Here, the researcher has briefly explained about how the excitement of electrons from the valence band after

absorbing sufficient energy from the sunlight to conduction band and to be involve in the reaction.

2.4 Doping

On the contrary, it is also due to the large bandgap of TiO_2 features, the utilization of the sunlight is very low. Which is also why doping is introduced to photocatalyst. Asahi et al (2001) first doped nitrogen into the TiO_2 which resulted in the increase of photocatalytic activity in the degradation of methylene blue (MB). They concluded that substitutional N doping causes bandgap narrowing through N 2p orbitals mixing with O 2p orbitals and their synthesized photocatalyst had shown to be activated under wavelength of 500 nm, which is in the visible light region. Ihara et al (2002) further explained that oxygen-deficient sites formed in grain boundaries are important to emerge vis-activity, and nitrogen doped in the part of oxygen-deficient sites are important as a blocker for reoxidation This is suggesting that the synthesized photocatalyst is using a great portion of the sunlight to carry out the reaction while having the sufficient negative redox potential to carry out the degradation of MB despite the bandgap being narrowed. Hence, at here, the researcher of the proposed study wants to point out that, the development of the photocatalyst is not all about being photosensitive to bring the TiO_2 to the visible light region yet to have sufficient energy to be photoexcited of an appropriate bandgap to carry out a certain specific reaction. This will lead to a vast developing of varied photocatalyst.

After the success of doping nitrogen to the TiO_2, a lot of doping had been done throughout the world, ranging from non-metal, for example, sulphur (Liu et al, 2007), carbon (Wang et al, 2007), silica (Periyat et al, 2008), to metal, such as ferum (Tieng et al, 2011), vanadium (Li et al,

2010), lanthanum (Wen et al, 2003), copper (Yoong et al, 2009), platinum, gold, and silver were reported as well by Peng et al (2012). To further increase the effectiveness of the doping, co-doping had been introduced which served as a promising approach (Liu et al, 2008). Co-doping, like nitrogen and sulphur (Wei et al, 2007), bismuth and boron (Bagwasi et al, 2013), sulphur and iron (Niu et al, 2013), carbon and iron (Wu et al, 2010). There are certainly a lot more of the experiments regarding doping on TiO_2 to list on. All of the researches give a significant bandgap narrowing as well as being photosensitive.

Among all, however, what catches the attention of the researcher is the copper doping. Copper is one of the metal, which does not go under oxidation easily (Wu et al, 2008). Of course, the fact of using noble metals is taken as consideration by the researcher, however, considering how expensive of those noble metals, therefore copper is taken as a choice as dopant.

2.5 Kinetic Studies of Methylene Blue (MB) Degradation

Here the reaction modeling of the MB degradation modeling will be reviewed. The modeling is done as to characterize the reaction itself with an equation so that the reaction can be predictable under various operating condition. This modeling is important also as to provide the design equation to design the photocatalytic reactor, where the equation on the rate of reaction is needed in order to design the volume of the continuous reactor or the reaction time as for the batch reactor.

In 2013, a model has been proposed by Sannino et al (2013) to model a reaction considering the concentration of the MB at that time, the

intensity of the light and the weight of the catalyst used. Hence a MB mass balance has been written as follows:

$$V \cdot \frac{dC(t)}{dt} = r(C, I) \cdot W_{\mathrm{TD}}$$

Here the V is the solution volume (L). C(t) is the MB concentration (mgL^{-1}). *r* is the reaction rate ($gL^{-1}min^{-1}$). W_{TD} is the catalyst amount (g). And I is the light intensity reaching the catalyst surface ($mWcm^{-2}$).

Later on, the mass balance is further modelling the methylene blue concentration and the intensity of the light with the Langmuir-Hinshelwood mechanism rate law. Then, the Lambert-Beer law is used to further models the intensity of the light in the form Langmuir-Hinshelwood mechanism rate law to consider the screening effect, where the penetration of light decreases when the catalyst loading is increasing. Hence, the rate of degradation of MB is written as follows:

$$V \cdot \frac{dC(t)}{dt} = -K_1 \cdot \frac{b \cdot C(t)}{1 + b \cdot C(t)} \cdot \frac{\alpha \cdot I_0 \cdot e^{-k_{\mathrm{I}} \cdot [\mathrm{TiO_2}]}}{1 + \alpha \cdot I_0 \cdot e^{-k_{\mathrm{I}} \cdot [\mathrm{TiO_2}]}} \cdot W_{\mathrm{TD}}$$

Where:

K_1 = Kinetic constant ($mg\ g^{-1}min^{-1}$)

α = Light absorption coefficient ($cm^2(mW)^{-1}$)

k_1 = Specific extinction coefficient per unit catalyst mass ($L\ mg^{-1}$)

I_0 = Light intensity incident on the reactor surface ($mW\ cm^{-2}$)

$[TiO_2]$ = Catalyst dosage ($mg\ L^{-1}$)

b = Adsorption coefficient ($L\ mg^{-1}$)

Still several weaknesses have been detected within this model. As mentioned before, the intensity of the light here has been modelled referring

to Langmuir-Hinshelwood mechanism rate law. As known, this Langmuir-Hinshelwood mechanism rate law is usually used to describe the reaction pathway of a catalytic reaction, where the reaction between two atoms is occurred when they are adsorbed on the surface of the catalyst as depicted as follows:

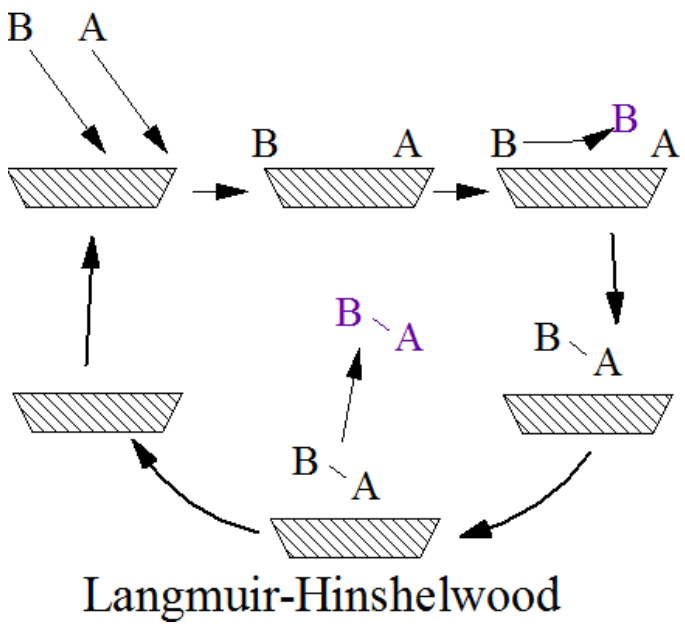

Figure 0.1: The reaction pathway of atoms as described by Langmuir-Hinshelwood mechanism rate law.

Hence, the doubt is raised when a rate law that characterize a reaction is used to model the effect of intensity of the light towards the degradation of the MB itself. Concrete evidence showing the incompatibility of the light intensity model is shown when we recalculate back the constant considering the light intensity using the value provided by Sannio et al (2013) as shown below that is used to model their degradation for catalyst weight 0.3 g and light intensity 32 $mWcm^{-1}$ in 100ml solution:

$\alpha = 0.000925\ cm^2\ (mW)^{-1}$

I_0 = 32 mWcm^{-1}

k_1 = 0.012 Lmg^{-1}

[TiO_2] = catalyst weight/ solution volume = 0.3 g/ 100 ml = 3000 mg/L

$$\frac{\alpha \times I_o \times e^{-k_1 \times [TiO_2]}}{1+\alpha \times I_o \times e^{-k_1 \times [TiO_2]}} = \frac{0.000925 \times 32 \times e^{-0.012 \times 3000}}{1+0.000925 \times 32 \times e^{-0.012 \times 3000}} = 6.87 \times 10^{-18}\ cm$$

This value suggested that after considering the light intensity factor for the degradation of MB itself, the rate of degradation MB is actually ranging around value of 10^{-18} cm, which is not in parallel with Sannio et al (2013) data. For the MB degradation with 0.3 g catalyst and light intensity 32 mWcm^{-1}, the data of MB concentration vs time is analysed and the graph of rate of MB degradation vs concentration of MB is generated using Origin software as shown in figure 2.3.

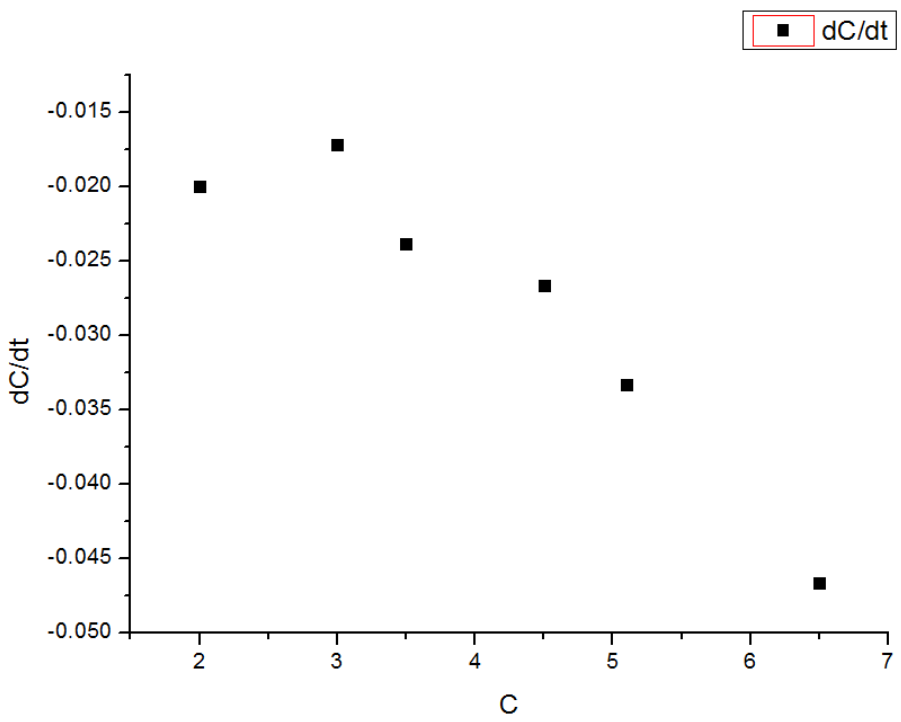

Figure 0.2: Graph of rate of MB degradation vs concentration of MB from Sannio et al (2013) data

As can be seen from the graph, the values of the rate of degradation are ranging around 0.075 $mgL^{-1}min^{-1}$ to 0.0475 $mgL^{-1}min^{-1}$. Looking back at the model proposed, if we replacing the remaining available constant back in to model (K_1 = 0.46 mg g^{-1} min^{-1}; b = 0.82L mg^{-1}; V = 100 mL; W_{TD} = 0.3 g; C_T = 2 mg/L to 6.5 mg/L), the rate of degradation obtained will be ranging around 10^{-18}, which is greatly deviating from the experimental data itself. Hence in this research, another model of equation had been explored to characterize our degradation of our MB which shown in chapter 4 later.

2.6 Summary

After surveying the literatures, to the author's best knowledge, therefore, the author had decided to use doping as a matter of increasing the photocatalytic activity and a proposed model equation is made.

3 MATERIALS AND METHODS

3.1 Overview

The copper salt is first synthesized before being doped into the synthesized TiO_2 to obtain the copper doped TiO_2. Characterization of the synthesized photocatalyst is followed. Lastly, the photocatalytic activity test is carried out with the degradation of the methylene blue.

3.2 Introduction

This part of the chapter will discuss on the procedures, along with the equipments on how the research is going to be conducted. The experiment can be divided into five sections as the following:

a) Preparation of Copper (Cu) Salt
b) Synthesis of Copper (Cu) Salt
c) Catalyst Preparation
d) Catalyst Characterization
e) Kinetic Study

3.3 Materials and Equipment

The materials that are used in the experiment are as followed:

- Acetic Acid (Sigma Aldrich Company)
- Ethanol 99.8% (Sigma Aldrich Company)
- Deionized Water
- Hydrazine Hydrate 64.5% (Sigma Aldrich Company)
- Copper-n-butoxide (Sigma Aldrich Company)
- Copper Nitrate (Sigma Aldrich Company)

- Ascorbic Acid (Sigma Aldrich Company)
- Glycerol

The equipments that are used in the experiment are:

- Oven
- Glass Furnace
- Hot Magnetic Plat Stirrer
- UV-vis spectrophotometre
- Batch reactor
- Water Cooling System
- Black Box
- High Intensity Lamp
- Centrifuge

The minor apparatuses that are used during the experiment:

- 250 mL beaker
- Weighing board
- Thermometer
- 5 mL measuring cylinder
- 50 mL beaker
- Parafilm
- 100 mL beaker
- 100 mL measuring cylinder
- Crucible
- Weigh balancer

- Mortar
- Magnetic rod
- 50 mL Centrifuge tube

Before the experiment is carried out, all of the minor apparatuses (except for parafilm) are rinsed with weak nitrate acid and dried in the oven for an hour to prevent any contamination.

The programmes used to study the kinetic study are:

- OriginPro 8
- Microsoft Excel 2007

3.4 Preparation of Copper (Cu) Salt

Two mixtures will be made before they are being mixed to prepare the Cu salt, addressing both mixtures mixture A and mixture B respectively.

3.4.1 Preparation of Mixture A

1. 50 mL of glycerol is measured in a 250 mL beaker.

↓

2. 10 mg of $Cu(NO_3)$ is weighed in the weighing board and mixed with the glycerol under magnetic stirring.

↓

3. The mixture is heated up to 85 ^{o}C and stopped, and left to cool down to the surrounding temperature.

3.4.2 Preparation of Mixture B

1. 10 mL of ethanol is measured using the 45 mL centrifuge tube.

↓

2. 6 mL of hydrazine is measured using pipette and mixed with ethanol.

↓

3. The mixture B is shook vigorously and the colour of the mixture will turn into light brown.

3.4.3 Synthesis of Cu salt

1. 10 mL of mixture A is measured using a 50 mL beaker.

↓

2. 6 mL of mixture B is measured using a 5 mL measuring cylinder.

↓

3. Both 10 mL of mixture A and 6 mL of mixture B are mixed together in a 250 mL beaker.

↓

4. The 250 mL beaker is sealed tight with parafilm.

↓

5. The mixture is mixed under magnetic stirring for 12 hours.

The colour of the resulted Cu salt is turned into red wine coloured after 12 hours of stirring.

3.5 Preparation of Copper (Cu) Doped TiO_2

The preparation of the Cu doped TiO_2 is carried by sol-gel method. Similarly, two mixtures are made first before both of them are mixed together. Both the mixtures are addressed as mixture C and D respectively.

3.5.1 Preparation of Mixture C

1. 20 mL of titanium-n-butoxide is measured with a 100 mL beaker.

↓

2. 4 mL of acetic acid is measured with a 5 mL measuring cylinder.

↓

3. 26 mL of ethanol is measured with 100 mL measuring cylinder.

3.5.2 Preparation of Mixture D

1. 8 mL of deionized water is measured with a 5 mL measuring cylinder.

↓

2. 12 mL of ethanol is measured with a 100 measuring cylinder.

↓

3. 12 mL of acetic acid is measured with a 5 mL measuring cylinder.

↓

4. 1.98 g of Cu salt is weighed.

↓

↓

4. The measured titanium-n-butoxide and the measured acetic acid are mixed together with the measured ethanol in a 250 mL beaker under magnetic stirring for 30 minutes.

5. The measured deionized water, the measured ethanol, and the weighed Cu salt are mixed together with the measured acetic acid in a 250 mL beaker under magnetic stirring for 30 minutes.

3.5.3 Synthesis of Cu Doped TiO_2

1. Mixture D is added to mixture C in a drop-wise manner for 30 minutes under magnetic stirring.

↓

2. The obtained mixture is sealed and stirred for another 30 minutes.

↓

3, The resultant gel is aged for another 24 hours and dried in an oven for 36 hours.

↓

The photocatalytic activity test is evaluated by the degradation of

4. The dried gel is grinded into powder form.

↓

5. The powdered gel is heat-treated in the glass furnace at 300 ^{o}C for 1 hour.

500 ppm of Methylene Blue (MB) is prepared as a stock solution for the photocatalytic test.

1. 500 mg of Methylene Blue (MB) is weighed on a weighing board.

↓

2. The MB is put into a 1 L volumetric flask and to be filled with deionized water until the 1 L level is topped up.

3.6.2 Preparation of Methylene Blue (MB)

1. 5 mL of Methylene Blue (MB) is taken from the stock MB and measured in a 100 mL measuring cylinder.

↓

2. The 5 mL of MB is diluted with deionized water and being topped up until 50 mL

↓

3. The concentration of the MB is evaluated with UV-vis spectrophotometre and recorded.

3.6.3 Absorption-Desorption Equilibrium

1. The temperature of the cooling system of the batch reactor is started for 30 minutes and set at 25 ^{o}C.

↓

2. 1 g of the synthesized catalyst is weighed on a weighing board.

↓

3. The synthesized catalyst is put into the batch reactor and mixed with the prepared MB under magnetic stirring for 2 hours inside a black box.

↓

4. The stirring is stopped and 1.5 mL of the MB is collected with a dropper and put into a centrifuge tube.

5. The centrifuge tube is centrifuged to separate the liquid MB with the synthesized catalyst.

3.6.4 Degradation of Methylene Blue (MB)

6. The concentration of the MB is evaluated with UV-vis spectrophotometre and recorded before it is mixed into the batch reactor again.

1. The neon lamp is switched on.

2. The concentration of the MB is collected for every 30 minutes interval and evaluated with UV-vis spectrometre after it is centrifuged before putting it back to the batch reactor.

↓

3. The concentration of the MB is recorded.

↓

4. The degradation of MB test is lasted for 2 hours.

↓

5. The C/C_0 is plotted against time, t.

3.7 Catalyst Characterization

The synthesized catalyst is brought to Universiti Kebangsaan Malaysia (UKM) with the aid of Madam Hamidah binti Abdullah for the FTIR to check whether Cu is dopped into the synthesized catalyst.

3.8 Kinetic Study

The kinetic of the reaction of the degradation of MB is studied, which utilised the knowledge of forward and backward finite-divided-difference formulas, and centered finite-divided-difference formula to evaluate the constant for the modeled equation (Sivalingam et al, 2003).

3.9 Summary

This chapter explained how the copper salt is made before being doped into TiO_2 to obtain the synthesized photocatalyst, along with the photocatalytic activity test and the kinetic study of the degradation of the MB.

4 RESULT AND DISCUSSION

4.1 Overview

The synthesized Cu doped TiO_2 is brought to UKM for the FTIR to check the existence of the Cu in the synthesized photocatalyst. The obtained result is being compared with the synthesized TiO_2. As for the kinetic study, the data obtained during the photocatalytic test was differentiated with the forward and backward finite-divided-difference formulas, and centered finite-divided-difference formula before being plotted. The constant for the modeled equation is evaluated.

4.2 Introduction

This chapter will discuss on the resulted obtained from the FTIR to inspect the existence of the Cu in the synthesized photocatalyst. It is later followed by the kinetic study of the degradation of MB.

4.3 Physical Appearance of Copper (Cu) Doped TiO_2

A comparison of the physical appearance of the synthesized Cu doped TiO_2 with the commercial TiO_2 is shown as below:

Figure 4.1: Synthesized Cu Doped TiO_2

Figure 4.2: Commercial TiO_2

The physical appearance of the synthesized Cu doped TiO_2 is mild orange, metallic in coloured (Figure 4.1) as compared to the commercial TiO_2 (Figure 4.2). The mild orange, metallic of the synthesized photocatalyst suggests that the existence of Cu is inside of the TiO_2. To further inspect whether the Cu is doped into the TiO_2, FTIR is needed.

4.4 FTIR Result

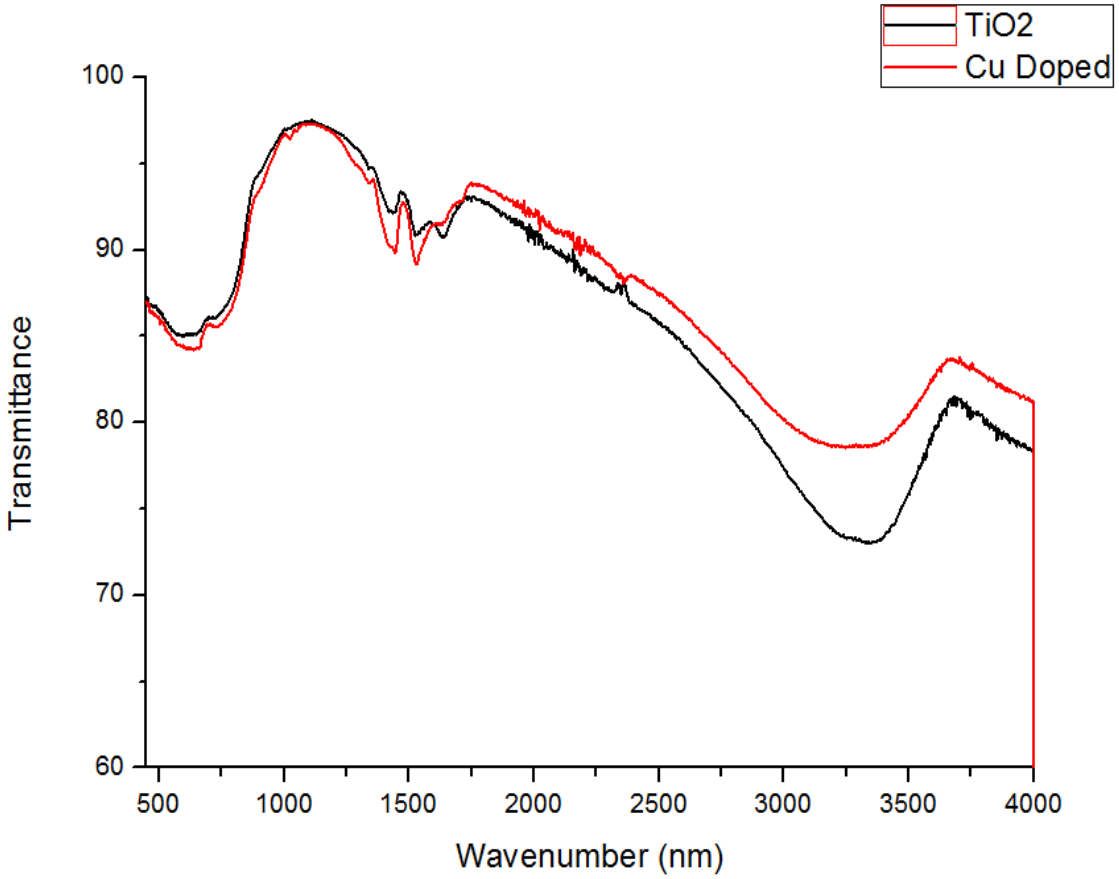

Figure 4.3: Comparison of the FTIR result of the synthesized Cu doped TiO_2 and the TiO_2

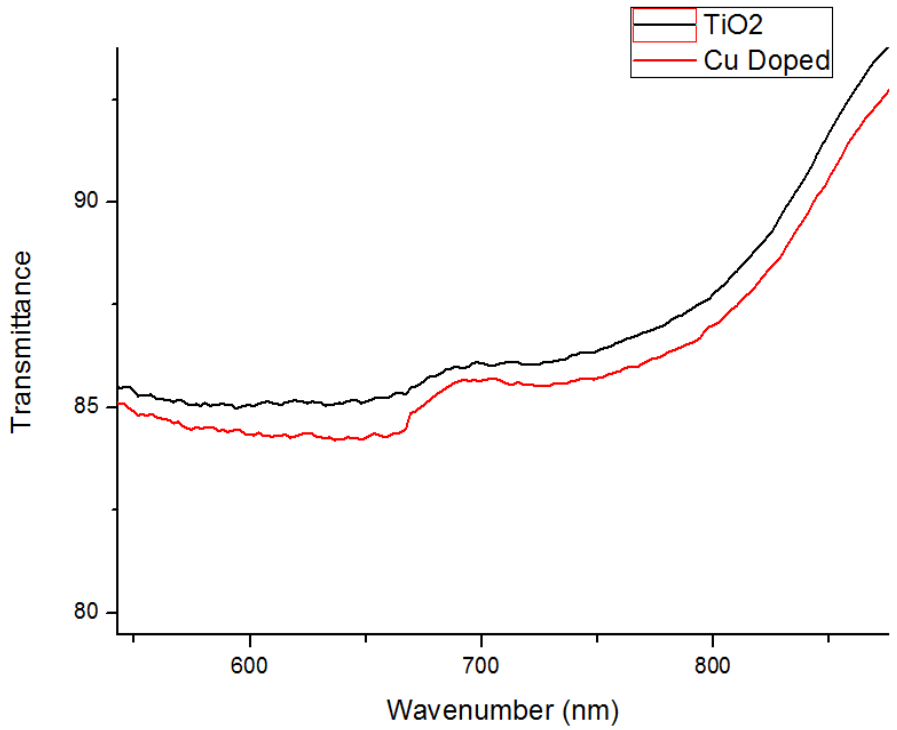

Figure 4.4: Comparison of the FTIR result of the synthesized Cu doped TiO_2 and the TiO_2 (Zoomed in)

The FTIR result of the synthesized Cu doped TiO_2 is being compared with the TiO_2. The wavenumber of the FTIR ranges from approximately 500 up to 4000 nm, while the transmittance ranges from 80 to 98. The most obvious changes is seen in the wavenumber ranges from 670 to 720 nm, where there is a new appearance of the bands in the synthesized Cu doped photocatalyst when compared to the TiO_2. According to Wang et al (2009) and Yan et al (2004) the new bands which appeared under the 1000 nm signified that the Cu is bonded with the O in the TiO_2. Therefore, Cu is successfully being doped into the synthesized photocatalyst.

4.5 Photocatalytic Activity Result

The synthesized Cu doped photocatalyst had been tested with the degradation of MB with 70, 50, and 30 ppm. The data collected from the photocatalytic activity is tabulated and plotted as below:

Table 4.1: Photocatalytic activity of synthesized Cu doped TiO_2 70 ppm MB

70 ppm MB

Time, t/ (min)	Concentration, C / mg/L	C/C_{01}	Percentage of Degradation of MB, %
0	69.99753	1	0
120	62.29780	0.890000	11.00000
150	38.91885	0.556003	44.39968
180	12.23699	0.174820	82.51797
210	5.55363	0.079340	92.06596
240	3.14761	0.044967	95.50326

Table 4.2: Photocatalytic activity of synthesized Cu doped TiO_2 50 ppm MB

50 ppm MB

Time, t/ (min)	Concentration, C / mg/L	C/C_{02}	Percentage of Degradation of

			MB, %
0	49.99946	1	0
120	48.14485	0.962907	3.70926
150	17.29485	0.345901	65.40993
180	7.138512	0.142772	85.72282
210	3.519126	0.070383	92.96167
240	1.273302	0.025466	97.45337

Table 4.3: Photocatalytic activity of synthesized Cu doped TiO_2 30 ppm MB 30 ppm

Time, t/ (min)	Concentration, C / mg/L	C/C_{03}	Percentage of Degradation of MB, %
0	29.87757	1	0
120	28.88711	0.966849	3.315069
150	8.935941	0.299085	70.09147
180	3.136476	0.104978	89.50224
210	1.261003	0.042206	95.77943
240	0.585478	0.019596	98.04041

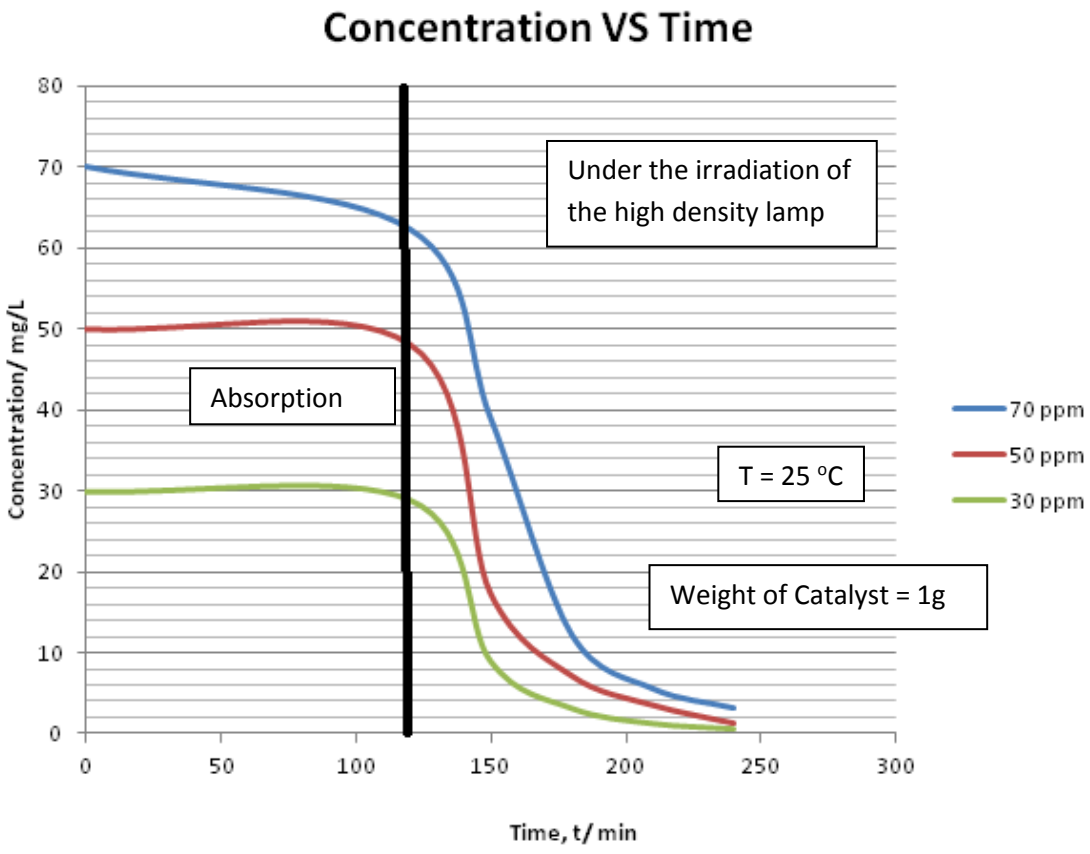

Figure 4.5: Concentration of 70, 50, and 30 ppm of MB versus time graph

The trend of the degradation of 70, 50, and 30 ppm of MB started with the relatively slow degradation at t = 0 min until t = 120 min, followed by a sharp decrease in the concentration of the MB until t = 200 min before the concentration became seemingly constant at the end of the experiment. The first slow degradation of the MB is due to absorption of the synthesized Cu doped TiO_2 which is responsible for the slight decrease in the MB concentration. At t = 120 min, when the high intensity lamp is turned on, the synthesized Cu doped TiO_2 started to get activated. Thus, in a very fast manner, the concentrations of all the 70, 50, and 30 ppm of MB had dropped significantly, approximately from 93% of its initial concentration down to 15% of its initial concentration in a matter of 2 hours time when t = 180 min.

The concentration came relatively constant after the time when t = 180 min before the photocatalytic activity test is stopped.

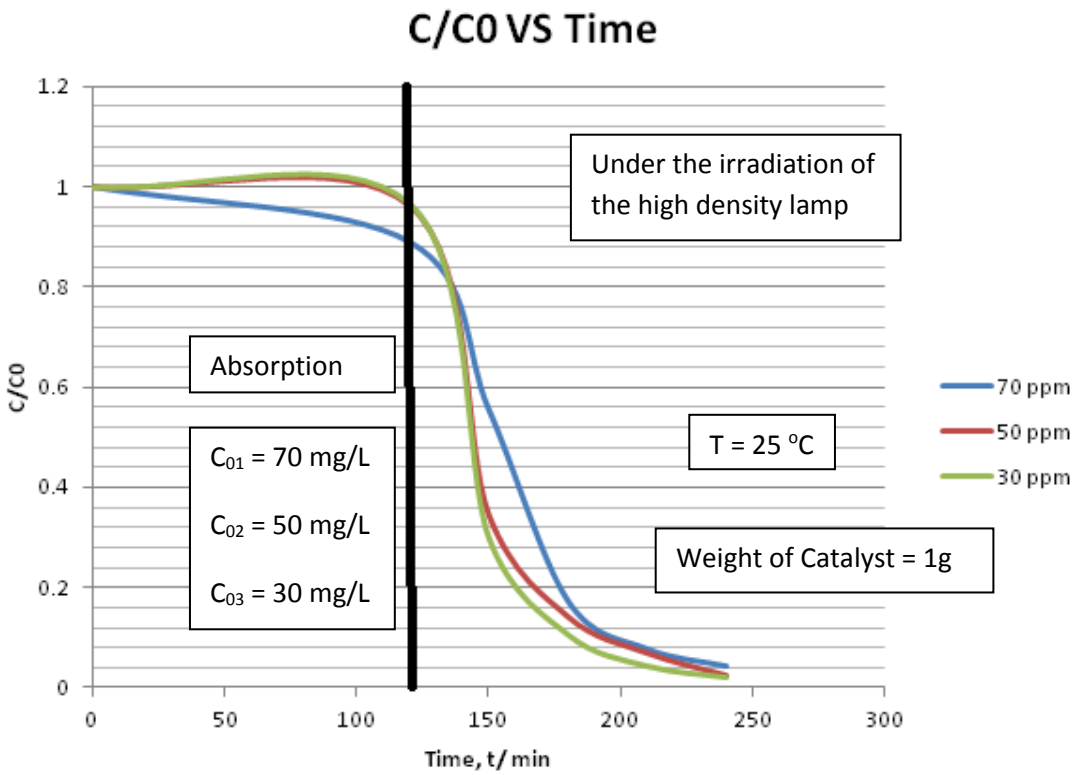

Figure 4.6: C/C_0 of 70, 50, and 30 ppm of MB versus time graph

Similar trend is observed in the C/C_0 versus time graph, where the degradation started slowly due to the absorption of the synthesized Cu doped TiO_2, followed by a sharp slope before they came to a relatively unchanged concentration before the end of the experiment.

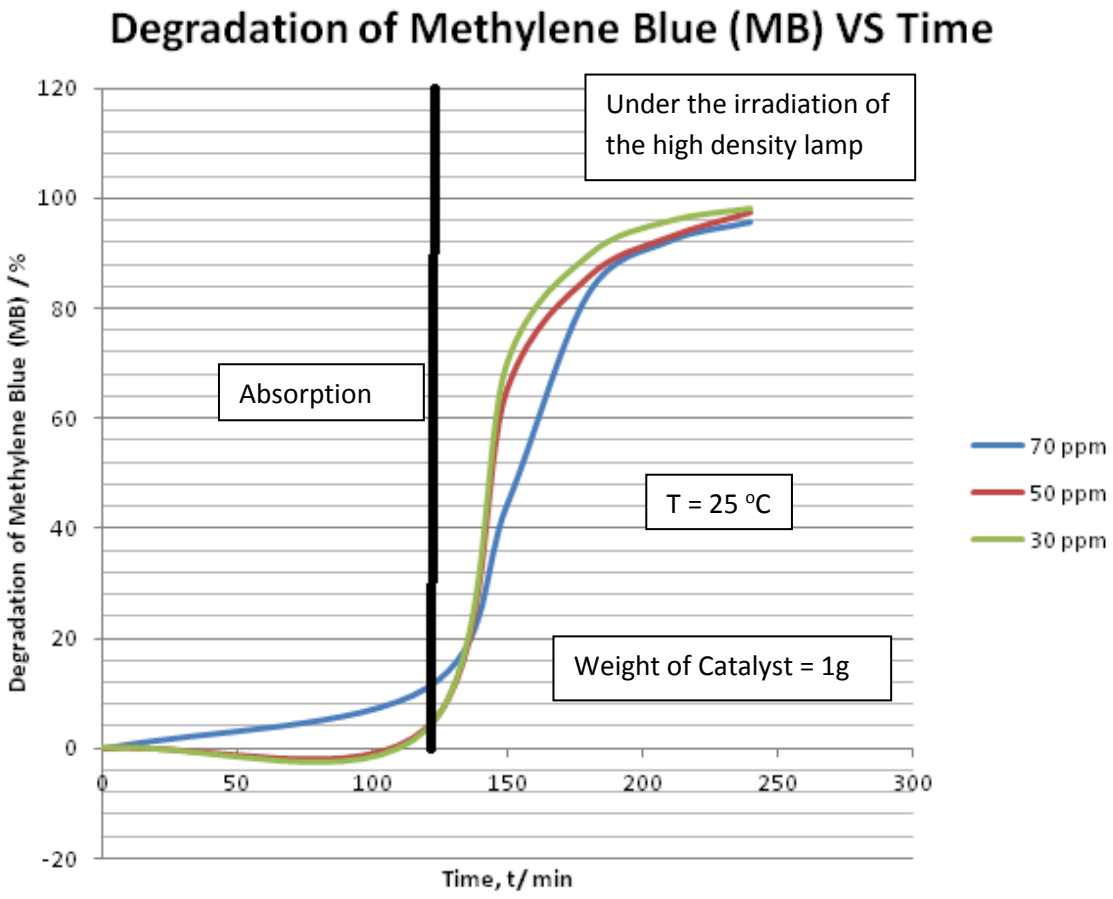

Figure 4.7: Percentage degradation of 70, 50, and 30 ppm of MB versus time graph

In this plot of degradation of MB versus time has the same trend as the previous two plots except that it is now in a reverse manner. This plot suggests that the degradation of the MB of 70, 50, and 30 ppm of MB increases when the lamp is turned on at t= 120 min until the reaction becomes slow when t = 180 min, which correlates with both of the previous plots.

4.5 Kinetic Study

The kinetics study of the degradation of MB is studied. The model used in this research takes account of the direct hole attack and the hydroxyl radical attack (Sivalingam et al, 2003).

In the reaction, the excitation of electron from the valence band to the conduction band has created hole after being irradiated under the sunlight,

$$TiO_2 + h\nu \xrightarrow{k_e} h_{VB}^{+} + e_{CB}^{-} \qquad \text{E.1}$$

k_e = reaction constant for this reaction.

At the same time, recombination of electrons will happen to generate the heat back as shown below:

$$h_{VB}^{+} + e_{CB}^{-} \xrightarrow{k_{rc}} \text{heat} \qquad \text{E.2}$$

k_{rc} = reaction constant for this reaction.

It is later followed by the hole generated, which will directly attack either the dye adsorbed on the surface of the catalyst, or the unbounded dye

in the solution to yield the cationic dye radicals. And the radicals produced will further react to get the end species as shown below:

$$S - D + h_{VB}^{+} \xrightarrow{k_{hr}^{a}} S - D^{0+} \rightarrow \text{end species} \qquad E.3$$

$$D + h_{VB}^{+} \xrightarrow{k_{hr}^{b}} D^{0+} \rightarrow \text{end species} \qquad E.4$$

The k^{a}_{hr} and k^{b}_{hr} are the reaction constants for both reactions respectively; S-D is the dye adsorbed on the catalyst surface; D is the unbounded dye in the solution; and D^{0+} is the cationic radical dye generated by direct hole attack.

Next the hydroxyl radical generation will be discussed. The hydroxyl radical can be generated via the attack of hole on the hydroxyl group or the water adsorbed on the surface of the catalyst as shown below:

$$S - H_2O + h_{VB}^{+} \underset{k'_{tr}}{\overset{k_{tr}}{\rightleftharpoons}} S - \dot{O}H + H^{+} \qquad E.6$$

$$S - OH^{-} + h_{VB}^{+} \underset{k'_{tr}}{\overset{k_{tr}}{\rightleftharpoons}} S - \dot{O}H \qquad E.5$$

The k_{tr} and k'_{tr} is the reaction constant for the forward and backward reaction of both reversible reactions. S-OH^{-} is the anionic hydroxyl group that adsorbed on the catalyst surface. S-H_2O is the water group that is

adsorbed on the catalyst surface. And S-OH· is the hydroxyl radical produced that is adsorbed on the surface.

Later, the adsorption and desorption of the mobile species in the reaction will be discussed. Here hydroxyl and dye can be adsorbed and desorbed away from surface of the catalyst as shown below:

$$S + D \underset{k'_D}{\overset{k_D}{\rightleftharpoons}} S - D, \quad K_D = \frac{k_D}{k'_D} \qquad E.7$$

$$S + \dot{O}H \underset{k'_{OH}}{\overset{k_{OH}}{\rightleftharpoons}} S - \dot{O}H, \quad K_{OH} = \frac{k_{OH}}{k'_{OH}} \qquad E.8$$

The k_D and k'_D is the reaction constant for the forward and backward reaction for E.8. And K_D is the equilibrium constant for the reaction E.7. While the k_{OH} and k'_{OH} is the reaction constant for the forward and backward reaction for E.8. And K_{OH} is the equilibrium constant for the reaction E.8

In the solution, since now both dye and hydroxyl radical is available either on catalyst surface or in the bulk, four possible combinations has been proposed where the reaction can occur: a) bounded hydroxyl radical and bounded dye; b) bounded hydroxyl radical and unbounded dye; c) unbounded hydroxyl radical and bounded dye; d) unbounded hydroxyl radical and unbounded dye as shown below:

Case (a):

$$S - D + S - \dot{O}H \xrightarrow{k_r^a} S + S - D'^{0} + M^{+}OH^{-} \qquad E.9$$

Case (b):

$$D + S - \dot{O}H \xrightarrow{k_r^b} S + D'^0 + M^+OH^- \rightarrow \text{end species} \qquad \text{E.10}$$

Case (c):

$$S - D + \dot{O}H \xrightarrow{k_r^c} S - D'^0 + M^+OH^- \rightarrow \text{end species} \qquad \text{E.11}$$

Case (d):

$$D + \dot{O}H \xrightarrow{k_r^d} D'^0 + M^+OH^- \rightarrow \text{end species} \qquad \text{E.12}$$

The k_r^a, k_r^b, k_r^c, k_r^d is the reaction constant for each reactions respectively. D'^0 is the cationic dye radical formed by hydroxyl radical attack. While the M^+ is the cation released from the dye molecule after being attack by hydroxyl radical.

Later on, relating the rate of disappearance of MB to the direct hole attack mechanism (E.3 and E.4) and hydroxyl radical attack (E.9, E.10, E.11, E.12):

$$\begin{aligned} -r_D = {} & k_{hr}^a[S-D][h_{VB}{}^+] + k_{hr}^b[D][h_{VB}{}^+] \\ & + k_r^a[S-D][S-\dot{O}H] + k_r^b[D][S-\dot{O}H] \\ & + k_r^c[S-D][\dot{O}H] + k_r^d[D][\dot{O}H] \end{aligned} \qquad \text{E.13}$$

In order to define E.13 in a measurable parameter [D], several concentration formulas have been formulated out. From E.7 and E.8, the concentration of [S-D] and [S-$\dot{O}$H] is further defined as follows:

$$[S-D] = K_D[S][D] \qquad \text{E.14}$$

$$[S-\dot{O}H] = K_{OH}[S][\dot{O}H] \qquad \text{E.15}$$

As to redefine [$\dot{O}$H], a total hydroxyl radical balance has been done from E.5, E.6, E.9, E.10, E.11, and E.12 as follows:

$$\begin{aligned}\frac{d([\dot{O}H]+[S-\dot{O}H])}{dt} &= k_{tr}[S-OH^-][h_{VB}{}^+] - k'_{tr}[S-\dot{O}H] \\ &\quad + k_{tr}[S-H_2O][h_{VB}{}^+] - k'_{tr}[S-\dot{O}H][H^+] \\ &\quad - k_r^a[S-\dot{O}H][S-D] - k_r^b[S-\dot{O}H][D] \\ &\quad - k_r^c[\dot{O}H][S-D] - k_r^d[\dot{O}H][D]\end{aligned} \qquad \text{E.16}$$

It is well known that normally in a batch reaction, the reaction is normally pccured in unsteady state manner. Still as to ease our calculation at this stage, a quasi steady state assumption (QSSA) is made as to further evaluating E.16:

$$\frac{d([\dot{O}H]+[S-\dot{O}H])}{dt} = 0$$

$$[\dot{O}H] = \frac{k_{tr}\{[S-OH^-]+[S-H_2O]\}[h_{VB}{}^+]}{K_{OH}\{k'_{tr}(1+[H^+])[S]+k_r^a[S-D][S] + k_r^b[D][S]\} + k_r^c[S-D] + k_r^d[D]} \qquad \text{E.17}$$

As to redefine $[h^{+}_{VB}]$, a hole concentration balance is also done from E.1, E.2, E.5, and E.6 as follows:

$$\begin{aligned}\frac{d[h_{VB}{}^{+}]}{dt} = {} & k_e[S] - k_{rc}[e_{CB}{}^{-}][h_{VB}{}^{+}] \\ & - k_{tr}[S - OH^{-}][h_{VB}{}^{+}] + k'_{tr}[S - \dot{O}H] \\ & - k_{tr}[S - H_2O][h_{VB}{}^{+}] \\ & + k'_{tr}[S - \dot{O}H][H^{+}]\end{aligned} \qquad \text{E.18}$$

Here, by assuming that the recombination process (E.2) is happening at faster rate as compared to other reaction and applying QSSA for E.18, E.18 can be further redefine to:

$$\frac{d[h_{VB}{}^{+}]}{dt} = 0$$

$$[h_{VB}{}^{+}] = \sqrt{\frac{k_e[S]}{k_{rc}}} \qquad \text{E.19}$$

Substituting E.14, E.15, E.17 and E.19 back into E.13, we will be getting:

$$-\frac{d[D]}{dt} = k_{0h}[D] + \frac{k_0 K_0[D]}{1 + K_0[D]} \qquad \text{E.20}$$

With the following constant that has been define along the substitution:

$$k_{0h} = k^{a}_{dch} + k^{b}_{dch}$$

$$k_0 = k_{dc} \quad \text{and} \quad K_0 = K^{a}_{DC} + K^{b}_{DC} + K^{c}_{DC} + K^{d}_{DC}$$

Parameters	Expressions
k^{a}_{dch}	$k^{a}_{hr} K_D [S] \sqrt{\frac{k_e [S]}{k_{rc}}}$
k^{a}_{dch}	$k^{b}_{hr} \sqrt{\frac{k_e [S]}{k_{rc}}}$
k_{dc}	$k_{tr} \{[S - OH^-] + [S - H_2O]\} \sqrt{\frac{k_e [S]}{k_{rc}}}$
K^{a}_{DC}	$\frac{k^{a}_{r} K_D [S]}{k'_{tr}(1 + [H^+])}$
K^{b}_{DC}	$\frac{k^{b}_{r}}{k'_{tr}(1 + [H^+])}$
K^{c}_{DC}	$\frac{k^{c}_{r} K_D}{K_{OH} k'_{tr}(1 + [H^+])}$
K^{d}_{DC}	$\frac{k^{d}_{r}}{K_{OH} k'_{tr}(1 + [H^+])}$

The k_{0h} is the overall rate constant for direct hole attack, k_0 is the overall rate constant for hydroxyl radical attack. Both constants are dependent on the reaction conditions and the catalyst properties, but they are independent of the nature of the dye used. K_0 is the adsorption equilibrium constant dependent on the characteristic of dye and the rate –determining step.

In Sivalingam et al (2003) works, all the parameters are evaluated using the initial rate method so that the effect of the intermediates on the degradation can be neglected. Hence from E.20, their formula is further derived as followed:

$$\frac{1}{r_{D0}} = \frac{1}{K_0((k_{0h}/K_0) + k_0)} \frac{1}{[D]_0} + \frac{1}{(k_{0h}/K_0) + k_0}$$

Instead of evaluating at the initial rate method and neglecting the effect of the intermediate towards the reaction, the model is fitted with the

data obtain along the time reaction as those effects are important also to be considered and to be characterized into the model. Hence, after reshuffling E.20,

$$\frac{-1}{r_{Dt}} = \frac{1}{K_0(\frac{k_{0h}}{K_0}+k_0)}\frac{1}{[D]_t} + \frac{1}{\frac{k_{0h}}{K_0}+k_0}$$

r_{Dt} = the rate of degradation of the MB at specific time. And $[D]_t$ is the concentration of the MB at the specific time.

From the Table 4.2, the concentration of the MB is differentiated with respect to time to obtain the rate of degradation of MB. A plot of -1/rate of MB degradation at specific time versus the concentration of the MB.

Table 4.4: Numerical differentiation of the degradation of MB

1/C	1/(rate)
0.020771	0.972447
0.057821	1.463188
0.140085	4.355488
0.284161	10.22981
0.78536	24.22850

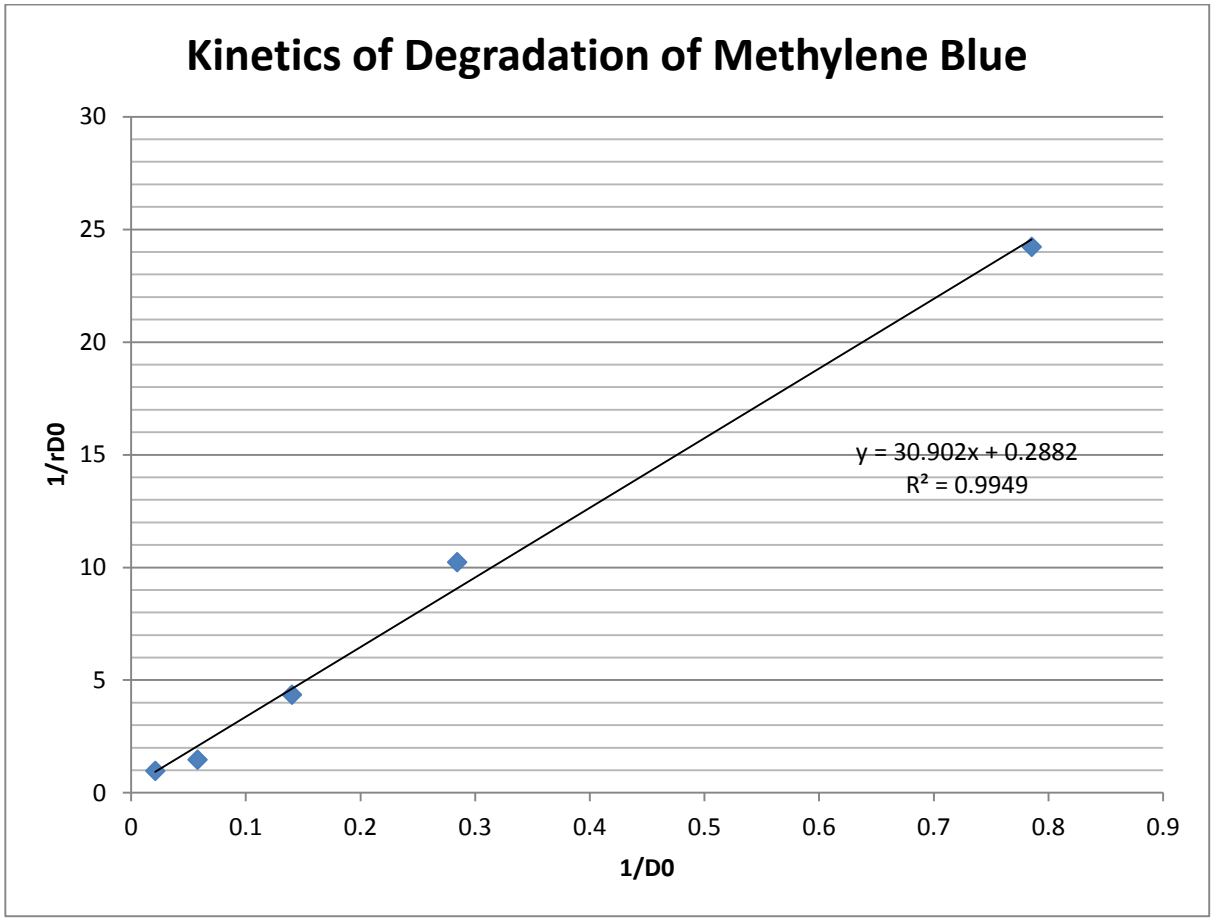

Figure 4.8: Kinetics of degradation of MB

The equation obtained from the experiment is y = 30.902x + 0.2882. The obtained $\frac{1}{K0\,((\frac{k0H}{K0})+k0)}$ constant is 30.902 while the obtained $\frac{1}{(\frac{k0H}{K0})+k0}$ is 0.2882, with a R^2 of 0.9949. Compared it to the linear equation obtained from Figure 4.8 with the model equation that proposed by Sivalingam et al (2003), the $K0\,((\frac{k0H}{K0}) + k0$ is 0.03236 mg L^{-1} min^{-1} while K_0 is 9.32615 X 10^{-3} ^{4}L mg^{-1}. According to Sivalingam et al (2003), the higher value of K_0 implies the blocking of the active sites of the catalyst due to strong adsorption, while the higher value of (k_{0h}/K_0+k_0) indicating the higher degradation rates of the dye.

4.7 Summary

The comparison of the synthesized photocatalyst with the commercial TiO_2 had been made. The existence of Cu had been further justified with the new bands that appeared in the region of less than 1000 nm. The increase in the photocatalystic activity is a success. The kinetic study of the degradation of MB had been studied.

5 CONCLUSION

5.1 Conclusion

The work of the research is a success and adhered to the objectives of the research. The doping of the Cu into TiO_2 is a success. The appearance of the new bands under the 1000 nm^{-1} signified that the Cu is bonded with the O in the TiO_2 (Wang et al, 2009; Yan et al, 2004). Therefore, the 1st objective is achieved. The 2nd objective is achieved as well, as there is an increased of photocatalytic activity of the synthesized photocatalyst in the methylene blue (MB) degradation test compared it to the commercial TiO_2. The kinetic of the degradation of Methylene Blue (MB) is studied, hence the 3rd objective is achieved.

5.2 Future works

The potential of the synthesized photocatalyst can be further demonstrated or to be further enhanced in the future. A few recommendations are given as below:

- More characterizations to be done onto the synthesized photocatalyst.

  Characterizations such as UV-Vis Spectrophotometer to obtain its bandgap, Brunauer-Emmett-Teller (BET) to check its surface area, Scanning Electron Microscope (SEM) for its morphologies, X-Ray Photoelectron Spectroscopy to further justified the Cu is doped into the TiO2, and X-Ray Diffractometer to check its crystal structure.

- Other forms of photocatalytic activities can be carried out with the synthesized photocatalyst.

  There are reports of utilising the other synthesized photocatalyst for other tests of photocatalytic activities. For example, Xu et al (2011),

Xu et al (2010), and Yoong et al (2009) who used their synthesized photocatalyst for the hydrogen production; Li et al (2008) and Wang et al (2006) for the degradation of methylene orange; Guan et al (2003) used it for reduction of carbon dioxide, Wu et al (2010) did it with the degradation of acid orange, phenol degradation by Liu et al (2007), eletrokinetic process by (Xiu et al, 2009), and many more.

- Codoped or doped with other elements in another method.

  Apart from sol-gel method, some other doping methods can be used as well. Ball milling technique was demonstrated by Chen et al (2005), vapor deposition by Yang et al (2004), reactive magnetron sputtering done by Wong et al (2005), precipitation-dipping method like what Li et al (2011) did, hydrothermal method by Wei et al (2007), and many other methods are available which proved to be an effective method of one way and another. Other elements doped into TiO_2 such as ferum (Guan et al, 2003), carbon (Park et al, 2009), nitrogen (Asahi et al, 2001; Chen et al, 2005; Yang et al, 2004; Wong et al, 2005), sulphur (Liu et al, 2007), tungsten (Saepurahman et al, 2010), and codoping like nitrogen and sulphur (Wei et al, 2007), lanthanum and iodine (Li et al, 2011), and many more, each of them have reported of their synthesized photocatalyst to be highly active.

- Other methods of calculating the kinetics can be used.

  To increase the accuracy of the numerical differentiation, methods as such the Runge-Kutta method can be applied.

- Glass furnace to be cleaned.

  The glass furnace used in the Faculty of Chemical Engineering & Natural Resources of Universiti Malaysia Pahang had been previously used by many other researchers, which left the glass furnace to be dirty. This would in return cause contaminations to any of the samples which kept in it during the calcination period. With the aid of the ventilating hot air medium would further increase the degree of contamination into the samples. A proper

cleaning should be done to reduce the degree of contamination of the samples, would thus provide a better study of the kinetic study.

References

Asahi, R. M. (2001). Visible-Light Photocatalysis in Nitrogen-Doped Titanium Oxides. *Science* , 269-271.

Bagwasi, S. T. (2013). Synthesis, Characterization, and Application of Bismuth and Boron Co-Doped TiO2: A Visible Light Active Photocatalyst. *Chemical Engineering Journal 217* , 108-118.

Bloh, J. Z. (2012). Designing Optimal Metal-Doped Photocatalysts: Correlationbetween Photocatalytic Activity, Doping Ratio, and Particle Size. *The Journal of Physical Chemistry* .

Chang, W. S. (2012). Visible Light–Responsive Core-Shell Structured In2O3@CaIn2O4 Photocatalyst with Superior Bactericidal Properties and Biocompatibility. *Nanomedicine:Nanotechnology,Biology,and Medicine* , 609-617.

Chen, H. H. (2012). Theoretical Investigation of the Metal-Doped SrTiO3 Photocatalysts for Water Splitting. *The Journal of Physical Chemistry C* , 7897-7903.

Dong, F. L. (2013). (NH4)2CO3 Mediated Hydrothermal Synthesis of N-Doped (BiO)2CO3 Hollow Nanoplates Microspheres as High-Performance and Durable Visible Light Photocatalyst for Air Cleaning. *Chemical Engineering Journal 214* , 198-207.

Guo, J. M. (2012). Highly Stable and Efficient Ag/AgCl@TiO2 Photocatalyst: Preparation Characterization, and Application in the Treatment of Aqueous Hazardous Pollutants. *Journal of Hazardous Materials 211– 212* , 77– 82.

Ihara, T. M. (2002). Visible-Light-Active Titanium Oxide Photocatalyst Realized by an Oxygen-Deficient Structure and by Nitrogen Doping. *Applied Catalysis B: Environmental 42* , 403-409.

Jiang, Z. X. (2012). Turning Carbon Dioxide into Fuel. *Phil. Trans. R. Soc. A* , 3343- 3364.

Kameyama, T., Taoda, H., Kimura, K., Nonami, T., and Takeuchi, K. (2010). Robust Science & Technology for Safe and Secure Life Space - Photocatalyst -. *National Institute of Advanced Industrial Science and Technology (AIST)* , 1-7.

Li, H. Z. (2010). Low Temperature Synthesis of Visible Light-Driven Vanadium Doped Titania Photocatalyst. *Journal of Colloid and Interface Science 344* , 247–250.

Liu, S. a. (2008). A Visible Light Response TiO2 Photocatalyst Realized by Cationic S- doping and its Application for Phenol Degradation. *Journal of Hazardous Materials 152* , 48-55.

Liu, W. J. (2011). Preparation, Characterization and Activity Evaluation of Ag2Mo4O13 Photocatalyst. *Journal of Hazardous Materials 186* , 2001- 2008.

Mills, A. a. (1997). An Overview of Semiconductor Photocatalysis. *Journal of Photochemistry and Photobiology* , 1-35.

Niu, Y. X. (2012). Visible Light Activated Sulphur and Iron Co-Doped TiO2 Photocatalyst for the Photocatalytic Degradation of Phenol. *Catalysis Today 201* , 159–166.

Periyat, P. B. (2008). High Temperature Stable Mesoporous Anatase TiO2 Photocatalyst Achieved by Silica Addition. *Applied Catalysis A: General 349* , 13-19.

Sano, T. M. (2012). Origin of Visible-Light Activity of N-Doped TiO2 Photocatalyst: Behaviors of N and S Atoms in a Wet N-Doping Process. *Applied Catalysis B: Environmental 128* , 77-83.

Shieh, K. L. (2006). Antibacterial Performance of Photocatalyst Thin Film Fabricatedby Defection Effect in Visible Light. *Nanomedicine: Nanotechnology, Biology, and Medicine 2* , 121– 126.

Tieng, S. K. (2011). New Homogeneously Doped Fe(III)–TiO2 Photocatalyst for Gaseous Pollutant Degradation. *Applied Catalysis A: General 399* , 191-197.

Wang, S., Xu, H., Qian, L., Jia, X., Wang, J., Liu, Y., and Tang, W. (2009). CTAB- Assisted Synthesis and Photocatalytic Property of CuO Hollow Miscrospheres. *Journal Solid State Chemistry*, 1088-1093.

Wang, X. M. (2007). Multi-Type Carbon Doping of TiO2 Photocatalyst. *Chemical Physics Letters 444* , 292-296.

Wei, F. N. (2008). Preparation and Characterization of N–S-Codoped TiO2 Photocatalyst and its Photocatalytic Activity. *Journal of Hazardous Materials 156* , 135-140.

Wen, C. D. (2006). Photocatalytic Activity Enhancing for TiO2 Photocatalyst by Doping with La. *Trans. Nonferrous Met. SOC. China 16* , 728-731.

Wu, Y. Z. (2010). Properties of Carbon and Iron Modified TiO2 Photocatalyst Synthesized at Low Temperature and Photodegradation of Acid Orange 7 under Visible Light. *Applied Surface Science 256* , 4260–4268.

Yan, X., He, J., Evans, D. G., Zhu, Y., and Duan, X. (2004). Preparation Characterization and Photocatalytic Activity of TiO2 formed from a Mesoporous Precursor. *Journal of Porous Materials*, 131-139.

Yoong, L. S. (2009). Development of Copper-Doped TiO2 Photocatalyst for Hydrogen Production under Visible Light. *Energy* , 1652–1661.

Yousef, A. B.-D. (2012). Influence of CdO-Doping on the Photoluminescence Properties of ZnO Nanofibers: Effective Visible Light Photocatalyst for Wastewater Treatment. *Journal ofLuminescence132* , 1668–1677.